J|A|C|S ARTICLES

Published on Web 11/05/2009

Active Sites in Graphene and the Mechanism of CO_2 Formation in Carbon Oxidation

Ljubisa R. Radovic*

Department of Energy and Mineral Engineering, The Pennsylvania State University, University Park, Pennsylvania 16802, and Department of Chemical Engineering, University of Concepción, Concepción, Chile

Received June 19, 2009; E-mail: lrr3@psu.edu

Abstract: Over the past decade we have witnessed a steady rise in contributions of computational quantum chemistry to the understanding of reactivity of carbon materials. Several litmus tests must be applied to this evolving body of work before it can be viewed with a sufficient degree of confidence. The results of a crucial test are presented here: formulation of thermodynamically and kinetically plausible paths for CO_2 formation in the deceivingly simple reaction $C + (1 - y/2)O_2 = (1 - y)CO_2 + yCO$. A mechanism is proposed that clarifies the nature of atoms responsible for adsorption and reaction of molecular oxygen on the surface of sp^2-hybridized carbons, both flat and curved, and is also consistent with the postulate that the (re)active sites are carbene- and carbyne-type carbon atoms at graphene edges. Using density functional theory and representative two-dimensional graphene clusters, a direct and an indirect route to CO_2 formation were identified as both necessary *and* sufficient to account for key experimental observations. The former involves single-site O_2 adsorption on carbene-type zigzag edges. The latter includes the presence of mobile epoxide-type oxygen on the basal plane and its insertion into an edge hexagon, analogous to the conversion of benzene oxide to oxepin; such "unzipping" of graphene and CO_2 desorption is favored at oxygen-saturated edges, thus accounting for the well-documented phenomenon of induced heterogeneity of carbon reactive sites.

1. Introduction

The most important fundamental issue in the surface chemistry and reactivity of sp^2-hybridized carbon materials, both flat and curved, is the exact "chemical" nature of the (re)active sites.[1,2] Active sites are those on which chemisorption of the reactive gas occurs, whereas at any given moment during reaction the reactive sites are those that participate directly in the formation of products; i.e., the former are both "spectators" and intermediates, whereas the latter are true reaction intermediates.

There are now close to 3000 published papers with the term "graphene" in their title (more than 1000 in the first nine months of 2009 alone!), most of them in physics journals and very few, if any, addressing this key issue. The litmus test for success in its resolution is consistency with a necessary *and* sufficient mechanism for the carbon−oxygen reaction, in which CO_2, and not only CO, is known to be a primary product. It is indeed astonishing that despite decades of mechanistic studies[3] it is still unknown how exactly CO_2 is formed during oxidation of carbon materials:

$$C + (1 - y/2)O_2 = (1 - y)CO_2 + yCO \qquad (1)$$

This is a reaction[1] of the greatest technological importance in energy and materials utilization both past and present (e.g., coal or biomass combustion and gasification, oxidation resistance of C/C composite materials, activated charcoal production); its relevance for the 21st century and beyond, in terms of energy efficiency, process effectiveness, and product selectivity, is tied at least to the purification[4] and surface modification[5] of carbon nanotubes or to O_2 reduction in carbon-based fuel cells.[6,7] Furthermore, because of the very high ratio of edge to basal-plane carbon atoms in the emerging graphene materials (e.g., graphene nanoribbons), the understanding and control of their chemistry is critically dependent on realistic models of edge reactivity.[8−10]

Molecular-level engineering of carbon-based "nanomaterials" cannot be successful until and unless this long-ignored issue is resolved or at least clarified. Thus, for example, Beran and co-workers used quantum chemistry to study oxygen adsorption on graphite, modeled as pyrene or coronene, and explored the possibilities of O_2 dissociation on basal plane sites[11,12] even

(1) Radovic, L. R. In *Encyclopedia of Materials: Science and Technology*; Buschow, K. H. J., Cahn, R. W., Flemings, M. C., Ilschner, B., Kramer, E. J., Mahajan, S., Eds.; Pergamon Press: Oxford, 2001, *975*−985.
(2) Radovic, L. R.; Bockrath, B. *J. Am. Chem. Soc.* **2005**, *127*, 5917–5927.
(3) Walker, P. L., Jr.; Taylor, R. L.; Ranish, J. M *Carbon* **1991**, *29*, 411–421.
(4) Ebbesen, T. W.; Ajayan, P. M.; Hiura, H.; Tanigaki, K. *Nature* **1994**, *367*, 519–519.
(5) Ajayan, P. M.; Ebbesen, T. W.; Ichihashi, T.; Iijima, S.; Tanigaki, K.; Hiura, H. *Nature* **1993**, *362*, 522–525.
(6) Yeager, E. *J. Mol. Catal.* **1986**, *38*, 5–25.
(7) Radovic, L. R. In *Carbon Materials for Electrochemical Energy Storage Systems*; Béguin, F., Frackowiak, E., Eds.; CRC Press: New York, 2009; pp *163*−219.
(8) Boukhvalov, D. W.; Katsnelson, M. I. *J. Am. Chem. Soc.* **2008**, *130*, 10697–10701.
(9) Boukhvalov, D. W.; Katsnelson, M. I. *J Phys Cond Matter* **2009**, *21*, 344205.
(10) Yu, S. S.; Zheng, W. T.; Jiang, Q. *IEEE Trans. Nanotechnol* **2008**, *7*, 628–635.

10.1021/ja904731q CCC: $40.75

though it had been well established experimentally[3,13] that this process occurs only on graphene edges. More recently, Yu et al.[10] used density functional theory (DFT) to study the oxidation of a graphene nanoribbon whose edges are also terminated with hydrogen atoms. They concluded that O_2 chemisorption is endothermic, contrary to the well-known experimental fact that, even at room temperature and on a great variety of carbon materials, it is highly exothermic. A more careful chemical identification of both active[3,13] and reactive[14,15] sites is necessary, especially regarding the presence and role of unpaired electrons; indeed, Lee and Cho[16] concluded recently that "more realistic modeling of [graphene nanoribbon] edge structure will be necessary to understand the experimental findings." This is arguably best accomplished using computational quantum chemistry by analyzing small but representative two-dimensional graphene clusters: the presence of adjacent graphene layers (at a distance of ca. 0.34 nm) is assumed to lead to second-order effects, whereas in many cases use of larger clusters or structures with periodic boundary conditions has led to qualitatively similar results. On the other hand, a key distinction between such clusters and polycyclic aromatic hydrocarbon (PAH) molecules is the experimental fact that not all edge sites in the former are necessarily saturated with hydrogen.[2]

2. Computational Methodology

Initial representative structures of graphene clusters were drawn either in ChemDraw or GaussView. Gaussian[17] computational experiments were carried out using DFT with the following keywords: opt freq b3lyp/6-31 g(d). This level of model chemistry is widely acknowledged to be a reasonable compromise between computational efficiency and the degree of mathematical approximation, especially regarding electron correlation. The spin multiplicity (M) in each case was either judiciously selected or varied over a reasonable range. (See Supporting Information for optimized geometries in terms of atomic coordinates and energies of each one of the clusters analyzed.) Of greatest interest here are the self-consistent field energies (ΔE), enthalpies (ΔH), and Gibbs free energies (ΔG) of these clusters and their reactions; values obtained at 298 K are used for meaningful comparisons. Mulliken charge distributions and spin densities are also informative; comparisons in a relative sense are again more important than absolute values, given the well-known limitations of this somewhat arbitrary formalism of electron density partition.

3. Results and Discussion

3.1. Proposed Model. Early and elegant isotope labeling studies[18] have demonstrated that CO_2 is a primary reaction product and not only a result of subsequent homogeneous CO oxidation. A reliable quantitative relationship between the CO-to-CO_2 ratio, i.e., the value of y in eq 1, and either reaction conditions or type of carbon material used (i.e., the size and degree of ordering of its graphene layers) does not exist yet.[1] The literature does contain many disparate clues; for example, it is known that y decreases with increasing oxygen surface coverage, which in turn is favored by low temperatures, high pressures, and high ratios of edge-to-basal-plane sites in the graphene layer.[1] However, heretofore there have been no concise mechanistic proposals that would be both sufficient *and* necessary to account for the majority of experimental observations. Using the venerable Occam's razor principle, such a mechanism should be equally applicable to all forms of sp^2-hybridized carbon materials, whether curved or flat: graphite, nanotubes, pyrolytic carbons, filamentous carbons, chars, cokes, activated carbons, soot, and perhaps even fullerenes. Here such a mechanism is presented (reactions 2−5 below) and substantiated. Its main distinguishing features are the clarification of different roles played by the three types of sites in graphene,[2] as well as the interconversion between spectators (temporarily stable surface complexes, $C_b(O)$) and reactive intermediates ($C_e(O)$). Sites C_{zz} and C_{ac} are at zigzag and armchair edges, C_e is an edge site (either zigzag or armchair), and C_b is a basal-plane site within the graphene layer.

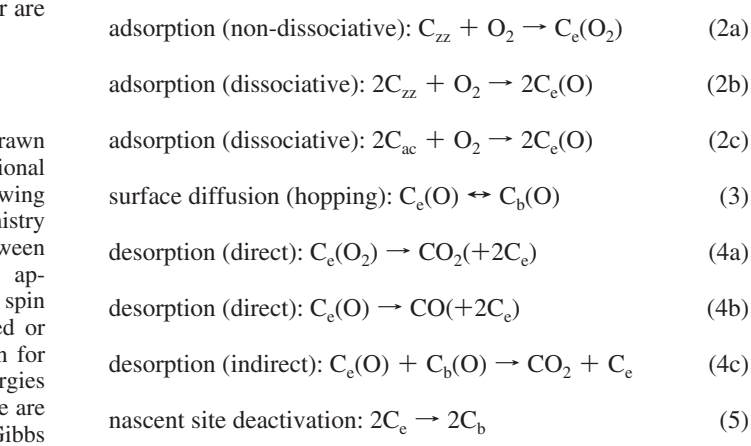

The nature and variety of edge sites is determined during the process of carbon formation: carbonization from the liquid or solid phase, or carbon nucleation and/or deposition from the gas phase.[19] This process is a balance between kinetically and thermodynamically limited elementary steps[20−22] that can be described succinctly as a growth of PAH species, predominantly fused benzene rings, whose principal characteristic is a competition between free-radical elimination of H (or of any other heteroatom) and achievement of the most stable ground state. Only two representative examples are presented here, as shown in Figure 1. For $C_{22}H_{12}$ the ground state is a triplet, loss of two H atoms results in a spin multiplicity (M) of five (four unpaired electrons), and exposure to O_2 results in the formation of two quinone-type surface groups; alternatively, loss of 4H results again in a structure with $M = 5$ rather than $M = 7$, by virtue of the formation of a carbyne-type[2] armchair pair. Its oxidative stabilization follows the same path as the loss of 2H. For $C_{19}H_{11}$ the ground state is a doublet, and loss of 1H results in a triplet-ground-state structure characterized by a carbene-like zigzag

(11) Beran, S.; Dubsky, J.; Slanina, Z. *Surf. Sci.* **1979**, *79*, 39–52.
(12) Dubsky, J.; Beran, S. *Surf. Sci.* **1979**, *79*, 53–62.
(13) Laine, N. R.; Vastola, F. J.; Walker, P., Jr. *J. Phys. Chem.* **1963**, *67*, 2030–2034.
(14) Radovic, L. R.; Walker, P. L., Jr.; Jenkins, R. G. *Fuel* **1983**, *62*, 849–856.
(15) Radovic, L. R.; Lizzio, A. A.; Jiang, H. In *Fundamental Issues in Control of Carbon Gasification Reactivity*; Lahaye, J., Ehrburger, P., Eds.; Kluwer Academic Publishers: Dordrecht, The Netherlands, 1991; pp 235−255.
(16) Lee, G.; Cho, K. *Phys. Rev. B* **2009**, *79*, 165440.
(17) Frisch, M. J. et al. *Gaussian 03*: Gaussian Inc.: Wallingford, CT, 2004.
(18) Walker Jr, P. L.; Vastola, F. J.; Hart, P. J. In *Fundamentals of Gas-Surface Interactions*; Saltsburg, H., Smith, J. N., Jr., Rogers, M., Eds.; Academic Press: New York, 1967; pp 307−317.
(19) Inagaki, M.; Radovic, L. R. *Carbon* **2002**, *40*, 2279–2282.
(20) Fitzer, E.; Mueller, K.; Schaefer, W. In *Chemistry and Physics of Carbon*; Walker, P. L., Jr., Ed.; Marcel Dekker: New York, 1971; Vol. 7, pp 237−383.
(21) Marsh, H.; Walker, P. L., Jr. In *Chemistry and Physics of Carbon*; Walker, P. L., Jr., Thrower, P. A., Eds.; Marcel Dekker: New York, 1979; Vol. 15, pp 229−286.
(22) Frenklach, M. *Phys. Chem. Chem. Phys.* **2002**, 2028–2037.

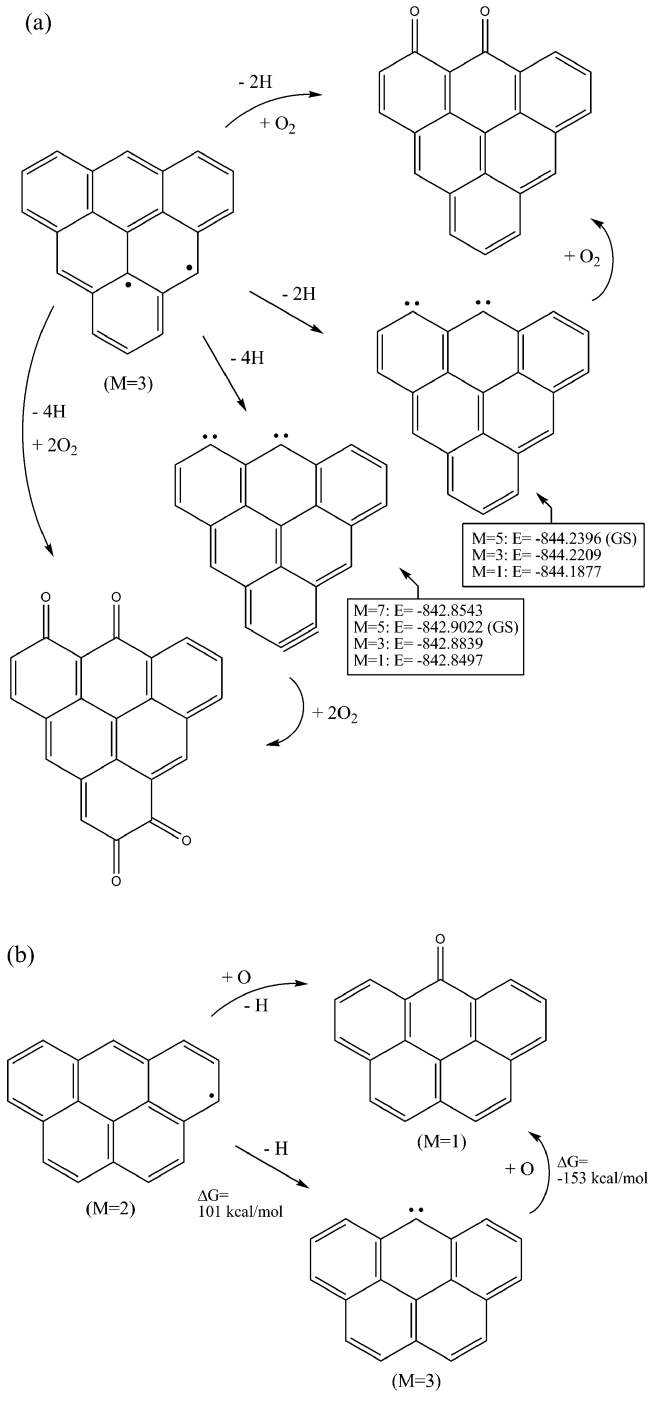

Figure 1. Fates of two representative PAH fragments during the (pyrolytic) process of carbon formation in inert and/or oxidative atmosphere: (a) $C_{22}H_{12}$ (triplet); (b) $C_{19}H_{11}$ (doublet). The SCF energy values shown are in hartrees.

site, whose further stabilization requires the presence of atomic oxygen. Such sites have been thoroughly characterized as intermediates in organic reactions,[23] and their relatively high stability (e.g., in room-temperature air) is a very fruitful postulate for graphenes.[2,24] An additional confirmation of its validity is the prediction that, as the size of graphene increases from one to four to nine hexagons (C_6H_4O to $C_{16}H_8O$ to $C_{30}H_{12}O$),[2] the enthalpy of adsorption of O_2 on the carbene site decreases from −57 to −34 to −16 kcal/mol.

Therefore, the chemically reactive sites in carbon materials, rather than being (as is too often assumed) either the very unstable unadulterated radicals formed by H removal from graphene edges or the very stable hydrogen-saturated graphene edges, are proposed to be an isolated carbene-type zigzag carbon atom and a carbyne-type armchair pair of carbon atoms. This hypothesis has been shown[2] to account for a remarkable variety of both "chemical" and "physical" experimental facts (e.g., unique amphoteric nature of carbon materials, positive thermoelectric power, and ferromagnetism); it is also consistent with the incisive intuitive arguments made by none other than Coulson half a century ago.[25]

3.2. Formation of Reactive Sites. Figure 2 illustrates the main possibilities of formation and fate of (re)active sites on carbon surfaces, and Table 1 establishes the thermochemical feasibility of these processes.

As is well known from PAH chemistry,[26] an odd number of hydrogen atoms terminating the fused benzene rings in graphene is the origin of the presence of an unpaired (and delocalized) π electron, which in turn is responsible for the paramagnetism of carbon materials.[27,28] When an edge site is not terminated with hydrogen, graphene stabilization likely occurs by formation of a carbene zigzag site (Figure 2a), with triplet being the ground state.[2] The fate of such an isolated zigzag site (site C_{zz} in reaction 2a) in wet oxidation is the formation of a phenolic group[29,30] and in dry oxidation it is postulated to be temporarily "non-dissociatively" adsorbed O_2. This single-site $C(O_2)$ intermediate is the precursor state in direct CO_2 formation during carbon oxidation, as discussed below; its existence is also consistent with the mechanism of electrochemical oxygen reduction.[6,7] An additional radical stabilization step in carbon oxidation is nascent site deactivation (NSD, Figure 2b).[2,31] Formation and entrapment of pentagons in such a process leads to curvature (and eventual fullerene formation); however, it is in competition with pentagon elimination (Figure 2c),[32] which preserves graphene planarity. The enthalpy changes of these two reactions are, respectively, −94.5 and −31.6 kcal/mol, and the corresponding entropy changes are −9 and −3 J/mol/K, in agreement with intuitive expectations.

The fate of two contiguous radical sites in an armchair configuration (Figure 2d) and of two adjacent radical sites in a zigzag configuration (Figure 2e) is the same: formation of quinone-type surface groups in dry O_2 and phenolic groups in wet oxidation, and the 2-electron interconversion of these two functionalities (quinone/hydroquinone equilibrium) is well documented in the carbon electrochemistry literature.[33] The nascent site deactivation (NSD) process in the case of armchair sites is very different from that of zigzag sites: the ground state

(23) Tomioka, H. In *Reactive Intermediate Chemistry*; Moss, R. A., Platz, M. S., Jones, M., Jr., Eds.; Wiley: New York, 2004; pp 376−395.
(24) Jones, J. M.; Jones, D. H. *Carbon* **2007**, *45*, 677–680.
(25) Coulson, C. A. In *Fourth Conference on Carbon*; Pergamon Press: Buffalo, NY, 1960; pp 215−219.
(26) Dias, J. R. *Mol. Phys.* **1990**, *30*, 251–256.
(27) Ingram, D.; Tapley, J.; Jackson, R.; Bond, R.; Murnaghan, A. *Nature* **1954**, *174*, 797–799.
(28) Zheng, S. K.; Feng, J.-W.; Maciel, G. *Energy Fuels* **2005**, *19*, 1201–1210.
(29) Boehm, H. P. *Carbon* **1994**, *32*, 759–769.
(30) Leon y Leon, C. A.; Radovic, L. R. In *Chemistry and Physics of Carbon*; Thrower, P. A., Ed.; Marcel Dekker, Inc.: New York, 1994; Vol. 24, pp 213−310.
(31) Radovic, L. R. In *Carbon Materials for Catalysis*; Figueiredo, J. L., Serp, P., Eds.; Wiley: New York, 2009; pp 1−44.
(32) Frenklach, M.; Moriarty, N. W.; Brown, N. *Proc. Combust. Inst.* **1998**, *27*, 1655–1661.
(33) Drushel, H. V.; Hallum, J. V. *J. Phys. Chem.* **1958**, *62*, 1502–1505.

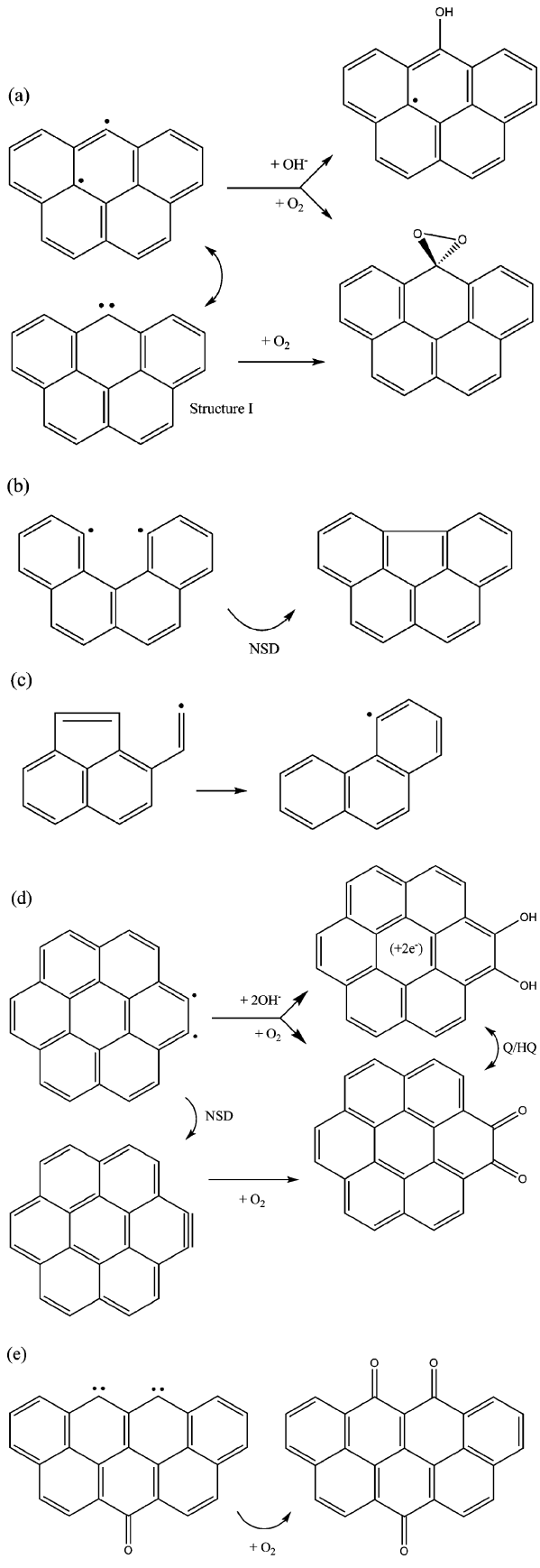

Figure 2. Prototypical reactions responsible for the formation of carbon active sites at graphene edges: (a) oxidation at (isolated) zigzag site; (b) deactivation of nascent active sites; (c) elimination of a pentagon; (d) oxidation at an armchair site (pair); (e) oxidation at adjacent zigzag sites.

Table 1. Free Energies of the Reactions Shown in Figure 2

panel of Figure *2*	reaction	ΔG, kcal/mol
(a)	$C_{19}H_{10}$ ($M = 3$) + $OH^- = C_{19}H_{10}OH$ ($M = 2$)	−98.1
	$C_{19}H_{10}$ ($M = 3$) + $O_2 = C_{19}H_{10}O_2$ ($M = 1$)	−50.1
(b)	$C_{18}H_{10}$ ($M = 3$) = $C_{18}H_{10}$ ($M = 1$)	−91.8
(c)	$C_{14}H_9$ ($M = 2$) = $C_{14}H_9$ ($M = 2$)	−30.6
(d)	$C_{24}H_{10}$ ($M = 3$) = $C_{24}H_{10}$ ($M = 1$)	−32.7
	$C_{24}H_{10}$ ($M = 3$) + $2OH^- = C_{24}H_{10}(OH)_2$ ($M = 1$)	−207
	$C_{24}H_{10}$ ($M = 3$) + $O_2 = C_{24}H_{10}O_2$ ($M = 1$)	−162
	$C_{24}H_{10}$ ($M = 1$) + $O_2 = C_{24}H_{10}O_2$ ($M = 1$)	−129
(e)	$C_{25}H_{10}O$ ($M = 5$) + $O_2 = C_{25}H_{10}O_3$ ($M = 1$)	−170

of the carbyne-type site[2] is a singlet, rather than a triplet. This provides a simple explanation for the persistent literature reports[2,34] of ferromagnetic behavior at zigzag edges.

It is clear from this analysis that structure I in Figure 2a is the only precursor state that can lead "directly" to CO_2 formation. Its existence, while consistent with isotope labeling studies,[18] also accounts for the heretofore intriguing report[35] that reaction of carbon with "oxygen-18 did not show complete statistical mixing of the isotopes in the CO_2 product, suggesting that a significant portion of the CO_2 product was formed by a direct reaction of surface carbon with molecular oxygen." An "indirect" route to CO_2 formation must also exist, however, because it is well known that dual-site, dissociative O_2 chemisorption is important in carbon reactions.[1,3] The decisive clue for postulating a plausible indirect route (see below) is a consequence of the fact[1,3] that more oxygen is often found on the carbon surface (especially for nongraphitic carbons such as chars, carbon blacks, and "amorphous" carbons) than can be accounted for by the concentration of edge sites.

3.3. Direct Route to CO_2. Figure 3 summarizes the proposed mechanism of CO_2 formation on the carbene-type zigzag sites. Such electrophilic oxidation is consistent with the charge and spin density distribution for this prototypical cluster, which is shown in Figure 4: even the relatively "unsophisticated" Mulliken population analysis clearly distinguishes between basal plane and edge sites and confirms the carbene nature of the reactive site (accumulation of ca. 1.4 electrons on site 10 in Figure 4b). The free energies of O_2 adsorption, oxygen desorption as CO_2, and nascent site deactivation are −50.1, 11.5, and −91.8 kcal/mol, respectively. The kinetics of this process will be discussed in detail elsewhere; suffice it to anticipate here that the activation energy of adsorption (step (i) → (ii)) is as low as ca. 20 kcal/mol (see Supporting Information, Figure S1, for the geometry of a typical transition state), which is well within the range of experimentally determined values for many carbon materials.[3,14,36]

3.4. Indirect Route to CO_2. It has long been known[13,14,37] that O_2 adsorption on basal plane sites does not lead to carbon gasification, and yet the existence of a mobile oxygen on the graphene surface,[38] i.e., oxygen that resides on a basal plane site but cannot directly produce CO or CO_2[38] by removing basal-

(34) Kopelevich, Y.; Esquinazi, P. *J. Low Temp. Phys.* **2007**, *146*, 629–639.
(35) Olander, D. R.; Jones, R. H.; Schwarz, J. A.; Siekhaus, W. J. *J. Chem. Phys.* **1972**, *57*, 421–433.
(36) Smith, I. W. *Fuel* **1978**, *57*, 409–414.
(37) Thomas, J. M. In *Chemistry and Physics of Carbon*; Walker, P. L., Jr., Ed.; Marcel Dekker: New York, 1965; Vol. 1, pp 121−202.
(38) Marsh, H. In *Oxygen in the Metal and Gaseous Fuel Industries*; Special Publication No. 32, First BOC Priestley Conference, Leeds, Sept. 1977; Chemical Society: London, 1978; pp 133−174.

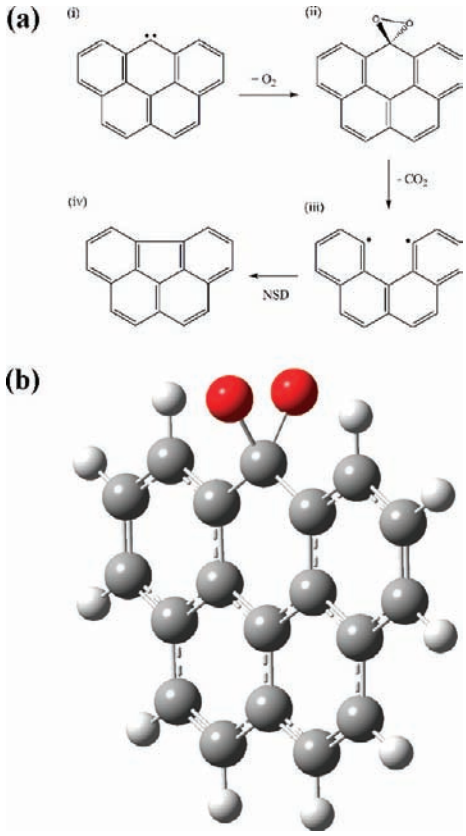

Figure 3. (a) Direct path to CO_2 formation at a carbene-type zigzag site: (i) $C_{19}H_{10}$ ($M = 3$), (ii) $C_{19}H_{10}O_2$ ($M = 1$); (iii) $C_{18}H_{10}$ ($M = 3$); (iv) $C_{18}H_{10}$ ($M = 1$). (b) Optimized geometry of $C_{19}H_{10}O_2$ ($M = 1$).

plane carbon atoms, is also well documented.[1,39,40] The process of formation of an epoxide-type oxygen on the basal plane is still an unresolved issue,[10,41−44] but circumstantial evidence for its presence there is compelling. It is not likely to occur as a consequence of O_2 interaction with two basal plane sites because O_2 has been shown to chemisorb dissociatively only at graphene edges.[3,37,45] Figure 5 summarizes one thermochemically feasible path to epoxy formation. Each one of these clusters is a ground state. It is noteworthy that structure 5d, containing a quinone and an epoxy-type oxygen, is more stable by some 30 kcal/mol than structure 5c (see Figure 3b), corresponding to oxygen adsorbed on the carbene site and in which the O−O bond distance is 0.15 nm (i.e., O_2 is not completely "dissociated"). The transition states connecting these stable structures will be discussed elsewhere.

The details of oxygen spillover, i.e., migration of oxygen atoms chemisorbed on graphene edge sites onto the basal plane,

(39) Yang, R. T.; Wong, C. *J. Chem. Phys.* **1981**, *75*, 4471–4476.
(40) Chen, S. G.; Yang, R. T.; Kapteijn, F.; Moulijn, J. A. *Ind. Eng. Chem. Res.* **1993**, *32*, 2835–2840.
(41) Chan, S.-P.; Chen, G.; Gong, X. G.; Liu, Z.-F. *Phys. Rev. Lett.* **2003**, *90*, 086403.
(42) Li, J.-L.; Kudin, K. N.; McAllister, M. J.; Prud'homme, R. K.; Aksay, I. A.; Car, R. *Phys. Rev. Lett.* **2006**, *96*, 176101.
(43) Sánchez, A.; Mondragón, F. *J. Phys. Chem. C* **2007**, *111*, 612–617.
(44) Orrego, J. F.; Zapata, F.; Truong, T. N.; Mondragón, F. *J. Phys. Chem. A* **2009**, *113*, 8415–8420.
(45) Yang, R. T. In *Chemistry and Physics of Carbon*; Thrower, P. A., Ed.; Marcel Dekker: New York, 1984; Vol. 19, pp 163−210.
(46) Skokova, K.; Radovic, L. R. In *Preprints of the 211th National Meeting, Div. Fuel Chem.*; American Chemical Society: Washington, DC, 1996; Vol. 41(1), pp 143−147.
(47) Hayes, D. M.; Nelson, S. D.; Garland, W. A.; Kollman, P. A. *J. Am. Chem. Soc.* **1980**, *102*, 1255–1262.

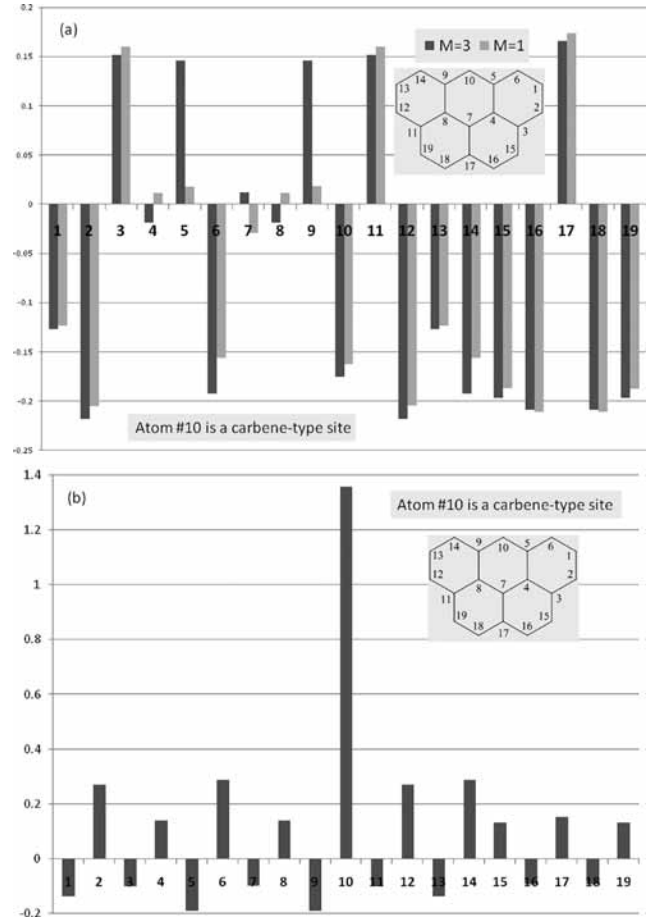

Figure 4. Mulliken population analysis of structure I (see Figure 2a): (a) charges; (b) spin densities of the triplet ground state.

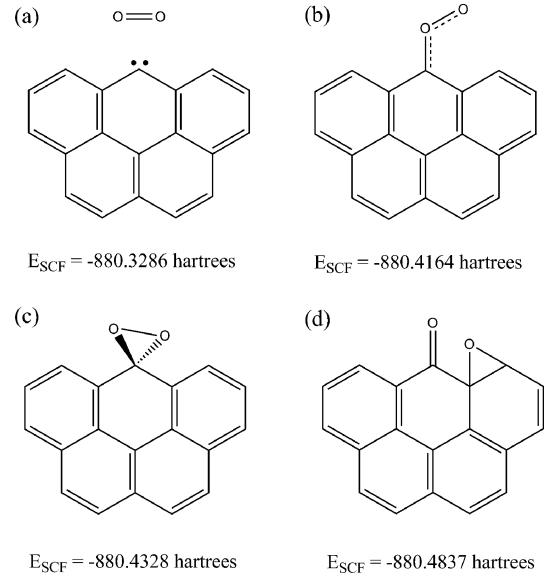

Figure 5. Selected thermodynamically stable graphene clusters ($C_{19}H_{10}$) that illustrate a likely path for the formation of an epoxide-type functionality on the graphene basal plane subsequent to O_2 chemisorption on a carbene-type edge site.

have yet to be clarified, but once there the fate of $C_b(O)$ turns out to be straightforward. Figure 6 illustrates a plausible pathway of CO_2 formation,[46] implicating epoxide-type oxygen, which is remarkably analogous to the well-known O-insertion mech-

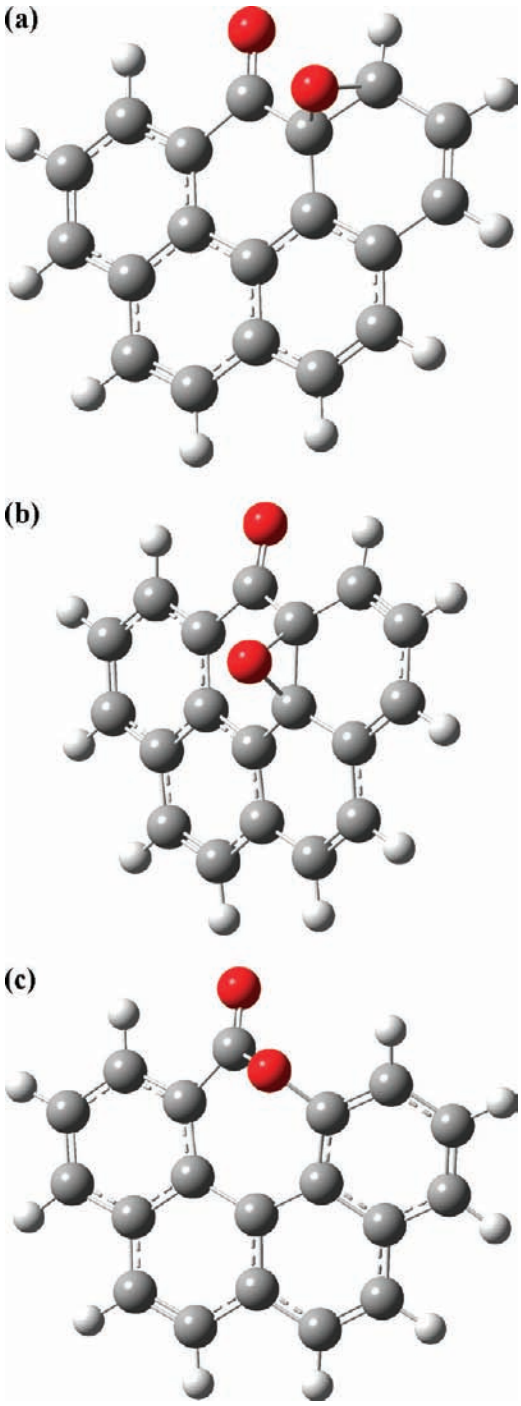

Figure 6. Optimized geometries of carbon clusters representing the indirect path to CO_2 formation: (a) $C_{19}H_{10}O(O1)$, $M = 1$; (b) $C_{19}H_{10}O(O_2)$, $M = 1$; (c) $C_{19}H_{10}O(O3)$, $M = 1$. For their SCF energies, see Supporting Information.

anism of oxepin/benzene oxide tautomerism.[47,48] Mondragón and co-workers[44] recently arrived at essentially the same conclusion in their analysis of oxidation of aromatic hydrocarbons with atomic oxygen.

Surface diffusion in carbon materials (represented somewhat simplistically as reaction 3) is a well-established concept, both experimentally[39,45,49] and theoretically.[39,49,50] The driving force,

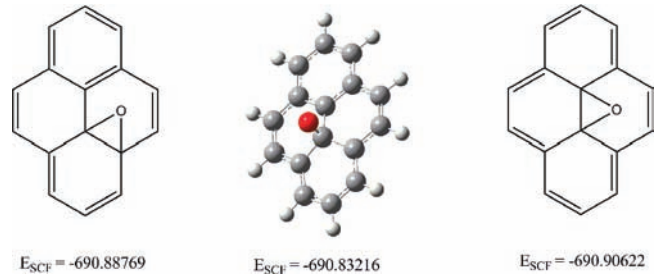

Figure 7. A mechanism for O-hopping (surface diffusion) on the graphene basal plane: (left) $C_{16}H_{10}(O1)$, $M = 1$; (middle) optimized geometry of the transition state; (right) $C_{16}H_{10}(O_2)$, $M = 1$. The energies shown are in hartrees.

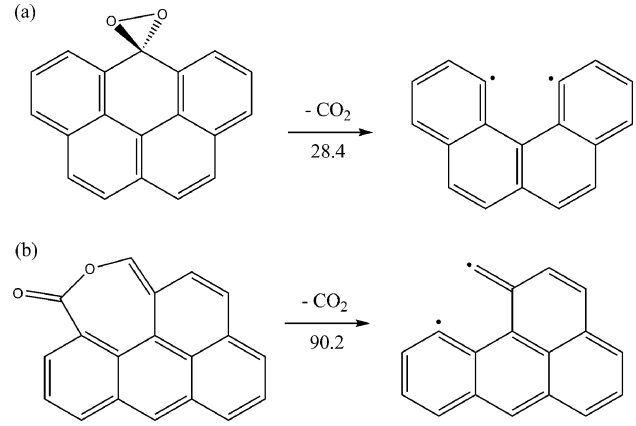

Figure 8. Thermochemistry of CO_2 desorption from two prototypical graphene clusters: (a) $C_{19}H_{10}O_2$ ($M = 1$) → $C_{18}H_{10}$ ($M = 3$) + CO_2 (direct route); (b) $C_{19}H_{10}O_2$ ($M = 1$) → $C_{18}H_{10}$ ($M = 3$) + CO_2 (indirect route). The ΔE values shown are in kcal/mol.

as well as the energetic barrier and the occurrence of "unzipping" of graphene,[42] depends on the details of electron distribution and requires further study. The main point of interest here is that there is no unzipping in Figure 6a and b: the epoxide C−C bond lengths are 0.151 and 0.155 nm, respectively. However, when the epoxy oxygen approaches the edge quinone-type site, its insertion does occur (Figure 6c); the epoxide C−C bond is 0.237 nm. The free energy of O insertion is −24.6 (Figure 6a) or −40.9 (Figure 6b) kcal/mol and that of subsequent desorption of CO_2 is 67.5 kcal/mol (vs 11.5 for direct CO_2 formation). As another example of a feasible mechanism, shown in Figure 7, hopping of epoxy oxygen in pyrene is energetically downhill (−11.0 kcal/mol) from the central to a peripheral bond, and the activation energy is ca. 35 kcal/mol; the transition state (Figure 7b) has the correct bond vibrational frequency (i720 cm^{-1}) with O on top of the C atom.

3.5. Product Desorption and the Role of Adsorbed Oxygen. Figures 8 and 9 summarize the most straightforward processes of CO_2 and CO desorption, subsequent to the initial adsorption of O_2 on carbon surfaces. The presence of dioxiranyl oxygen[51] (Figure 8a) is seen to be more advantageous for CO_2 formation than that of a cyclic ether (Figure 8b); the respective ΔG and ΔH changes are 11.5 vs 72.4 and 25.8 vs 85.7 kcal/mol.

(48) Pye, C. C.; Xidos, J. D.; Poirier, R. A.; Burnell, D. J. *J. Phys. Chem. A* **1997**, *101*, 3371–3376.
(49) Miessen, G.; Behrendt, F.; Deutschmann, O.; Warnatz, J. *Chemosphere* **2001**, *42*, 609–613.
(50) Hayns, M. R. *Theor. Chim. Acta.* **1975**, *39*, 61–74.
(51) Barckholtz, C.; Fadden, M. J.; Hadad, C. M. *J. Phys. Chem. A* **1999**, *103*, 8108–8117.

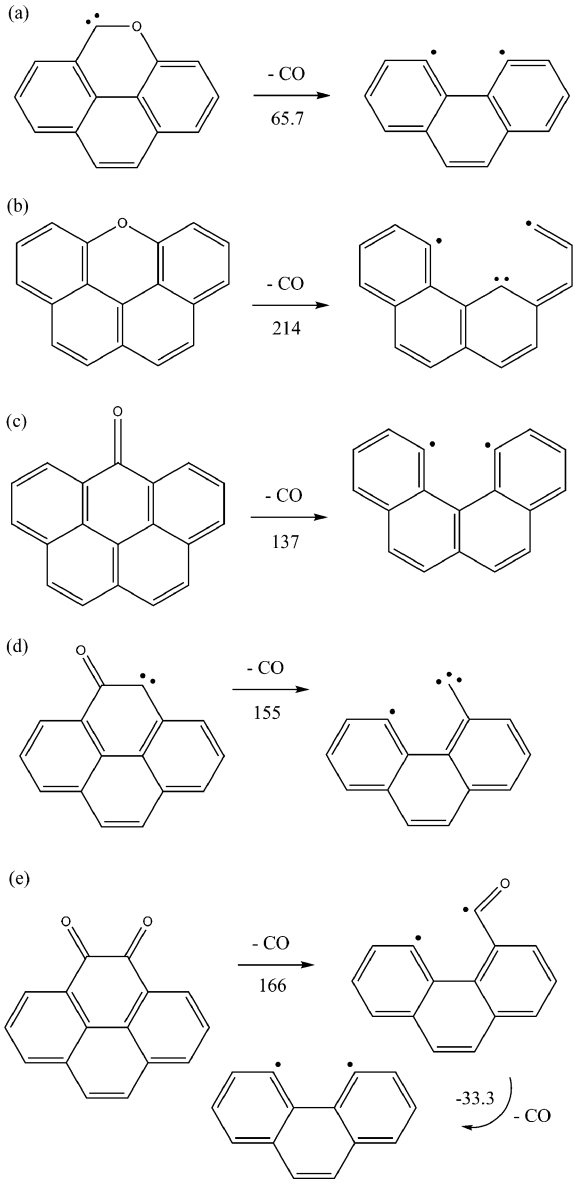

Figure 9. Thermochemistry of CO desorption from five prototypical graphene clusters: (a) $C_{15}H_8O$ ($M = 1$) → $C_{14}H_8$ ($M = 3$) + CO; (b) $C_{18}H_{10}O$ ($M = 1$) → $C_{17}H_{10}$ ($M = 5$) + CO; (c) $C_{19}H_{10}O$ ($M = 1$) → $C_{18}H_{10}$ ($M = 3$) + CO; (d) $C_{16}H_8O$ ($M = 3$) → $C_{15}H_8$ ($M = 5$) + CO; (e) $C_{16}H_8O_2$ ($M = 1$) → $C_{15}H_8O$ ($M = 5$) + CO; $C_{15}H_8O$ ($M = 5$) → $C_{14}H_8$ ($M = 1$) + CO. The ΔE values shown are in kcal/mol.

An armchair cyclic ether, contiguous to a carbene-type carbon (Figure 9a), is seen to be the preferred path to CO formation. The ground state of the cluster shown in Figure 9a is a singlet rather than a triplet (with $\Delta E_{S/T} = 21.1$ kcal/mol); the latter is more common when oxygen is absent from the ring system, e.g., in Figure 9d with $\Delta E_{S/T} = -15.3$ kcal/mol. Even for a larger such cluster, a six-ring $C_{21}H_{10}O$ (not shown), the thermodynamic barrier for CO desorption is relatively low, $\Delta E = 72$ kcal/mol. Its initial presence in oxygen-rich biomass-derived chars, as opposed to, say, coal-derived chars, may be responsible for their higher reactivity when compared with chars obtained from other precursors at the same heat-treatment temperature.

A zigzag cyclic ether[43] (Figure 9b) is seen to be an unlikely site for the initiation or propagation of CO desorption, whereas the decomposition of the most common quinone functionality at either zigzag (Figure 9c) or armchair sites (Figure 9d and e)

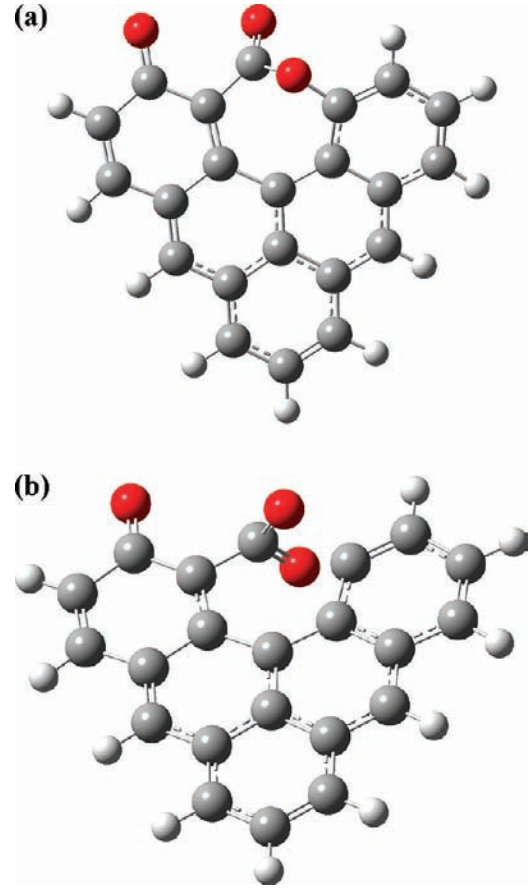

Figure 10. Optimized geometries of graphene cluster $C_{22}H_{10}O_3$ that illustrate the role of chemisorbed oxygen in lowering the activation energy of CO_2 desorption: (a) ground state ($M = 1$); (b) transition state ($M = 1$). See Supporting Information for their SCF energies.

exhibits an intermediate thermodynamic barrier. It is interesting to note, in agreement with intuitive expectations, that desorption of one CO molecule from an armchair site (Figure 9e), although quite endothermic, leads to a structure that only formally has two unpaired electrons; subsequent desorption of the other CO molecule is indeed exothermic. The ground state of $C_{15}H_8O$ is actually a quintet. The corresponding triplet state does not converge easily, even when force constants are calculated and quadratic convergence method is used.[52] Interestingly, however, the distance between the atoms with the unpaired electrons is much closer to that found for the singlet, 0.153 nm, than for the quintet, 0.291 nm. (The distribution of spin densities is shown in Figure S2; see Supporting Information.) This process of *nascent site deactivation* (see also Section 3.2) will be analyzed at length elsewhere. For the current discussion, it is sufficient to make a comparison of the distribution of spin densities in the intermediate product $C_{15}H_8O$ (Figure 9e; see also Figure S2a in Supporting Information) to that found for the product of desorption of CO from a graphene cluster containing a cyclic ether (Figure 9b), which also has four unpaired electrons but in a more intuitively obvious fashion (as indicated by the four dots in Figure 9b vs two dots in Figure 9e), and with the equally intuitive quintet structure in Figure 9d. In the latter two ($C_{17}H_{10}$ and $C_{15}H_8$) spin density is

(52) Frisch, A.; Frisch, M. J.; Trucks, M. *Gaussian 03 User's Reference*, 2nd ed.; Gaussian, Inc.: Wallingford, CT, 2005.

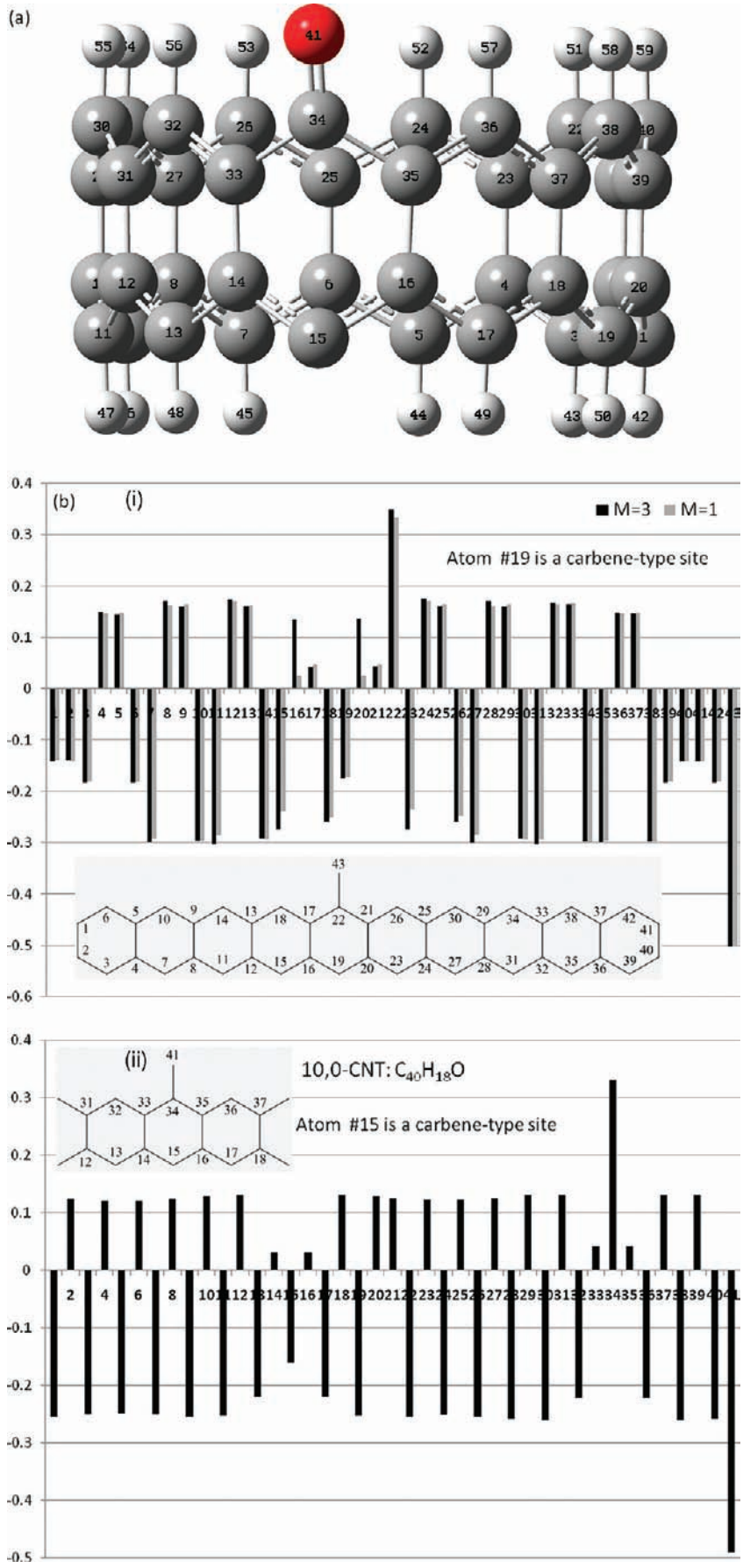

Figure 11. (a) Optimized geometry of the curved graphene cluster 10,0-CNT $C_{40}H_{18}O$ ($M = 1$) containing a zigzag active site. (b) Comparison of charge distributions in flat and curved graphene clusters containing a zigzag active site: (i) $C_{42}H_{22}O$; (ii) 10,0-CNT $C_{40}H_{18}O$ ($M = 1$).

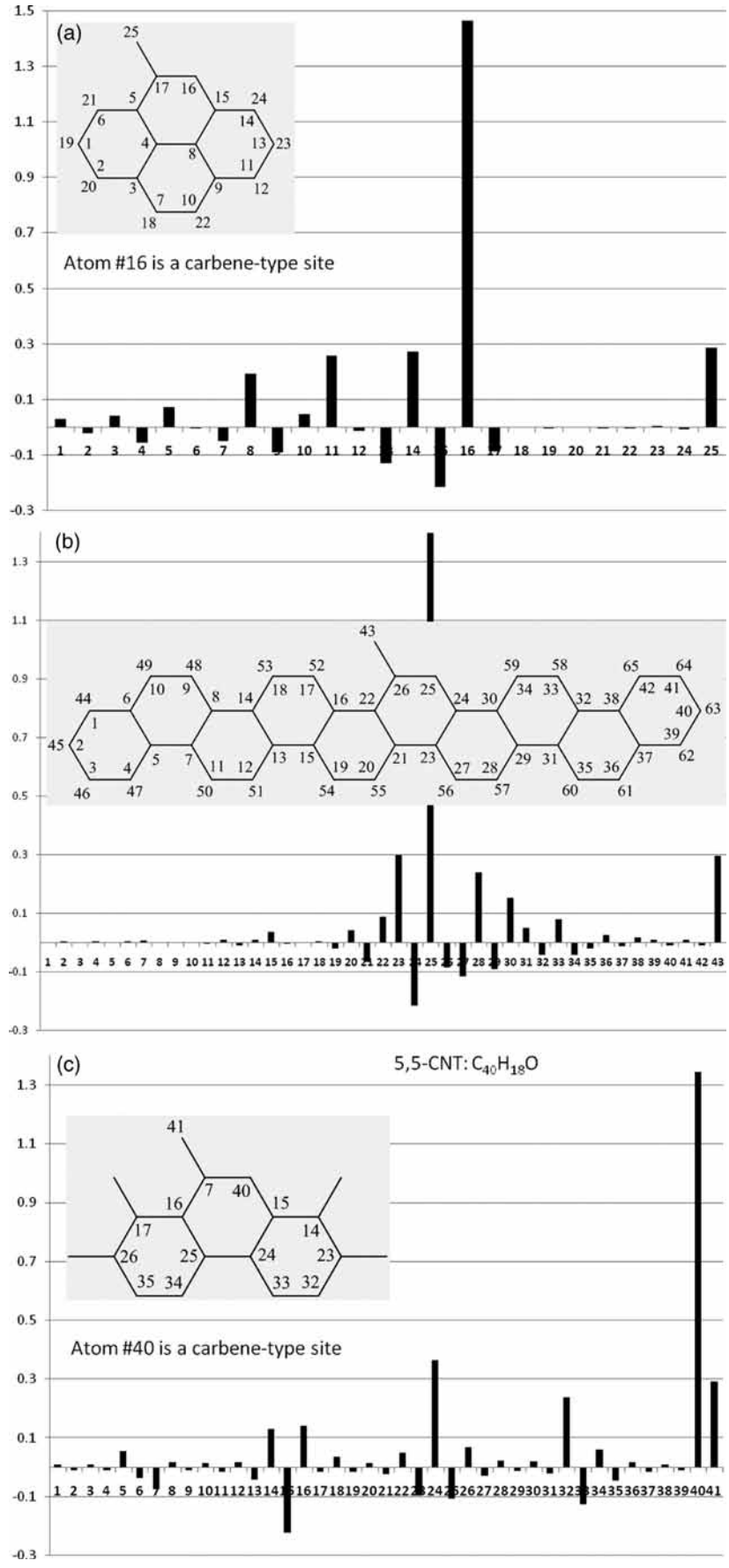

Figure 12. Comparison of spin densities in flat and curved graphene clusters containing an armchair active site: (a) $C_{16}H_8O$ ($M = 3$); (b) $C_{42}H_{22}O$ ($M = 3$); (c) 5,5-CNT $C_{40}H_{18}O$ ($M = 3$).

concentrated according to expectations, whereas in $C_{15}H_8O$ the unpaired electrons are more delocalized.

The power of computational quantum chemistry is most clearly displayed in the analysis of induced energetic heterogeneity of reactive sites in graphene.[1] It has long been known that, upon accumulation of surface oxygen, there is a change in both the reactivity and the number of active sites, but their experimental quantification has been elusive. A prototypical example is analyzed here. In Figures 6 and 8b the indirect pathway (reactions 2b, 2c, 3, and 4c) to CO_2 was illustrated, analogous to O-insertion mechanism in the conversion of benzene oxide to oxepin.[48] Figure 10 illustrates the kinetics of the process for a graphene cluster. In the absence of the adjacent quinone group (for the reaction $C_{19}H_{10}O_2 = C_{18}H_{10} + CO_2$), the activation energy of CO_2 desorption is 193 kcal/mol, and in its presence (for the reaction $C_{22}H_{10}O_3 = C_{21}H_{10}O + CO_2$) it is lowered to 61 kcal/mol; the epoxide C−C bond length in this case (compare with Figure 6c) is 0.232 nm. This remarkable decrease in activation energy is consistent with the well-documented increase in the reactivity of carbon as its gasification proceeds.[15,53] It can also be used profitably to explain a wide variety of seemingly unrelated phenomena:[2] the effectiveness of coal hydrogasification vs hydropyrolysis,[54] O_2-enhanced NO reduction by carbons,[55,56] and the enhancement of hydrogasification reactivity of carbons by nitric acid treatment.[57]

3.6. Comparison of Flat and Curved Graphene Clusters. Using again the Occam's razor argument (see Section 3.1), there is no reason to assume that the (re)active sites in carbon nanotubes (CNTs), as well as the processes of O_2 adsorption on them and CO or CO_2 desorption from them, are substantially different from the ones presented above for flat graphene clusters. Thus, Figure 11 highlights the analogies between a flat and a curved graphene cluster containing a zigzag active site: the distinction between basal plane and edge sites in the 10,0-CNT (formed by "wrapping" the $C_{42}H_{22}O$ cluster at the C1−C2/C41−C40 edge) is qualitatively identical to that observed for the flat graphene cluster, as is the charge "perturbation" in the vicinity of the carbene-site-containing ring.

The same analogy holds true for the armchair sites. For the 5,5-CNT containing a carbene site contiguous to a cyclic ether oxygen ($C_{39}H_{18}O$) (compare with Figure 9a) singlet is the ground state, with $\Delta E_{S/T} = 24.0$ kcal/mol. In contrast, triplet is the ground state ($\Delta E_{S/T} = -10.2$ kcal/mol) for the 5,5-CNT with a carbene site (compare with Figure 9d) contiguous to a quinone oxygen functionality ($C_{40}H_{18}O$); the spin density distributions (Figure 12) show qualitatively and quantitatively comparable charge accumulation (ca. 1.3−1.5 electrons) on the carbene site in both flat and curved clusters.

The charge distribution for the armchair 5,5-CNT (see Supporting Information, Figure S3) highlights the similarities and some differences with respect to its zigzag isomer (Figure 11b). Apart from the clear distinction between basal plane and edge sites in both cases and the accumulation of charge at the quinone functionality, the ratio of average negative charge to average positive charge is three times smaller for the latter. Also, the zigzag CNT is less "stable" (by 10.6 kcal/mol) than the armchair CNT: their SCF energies are −1610.09865 and −1610.11549 hartrees.

Analysis of the singlet−triplet transitions in zigzag CNTs will be discussed in an upcoming publication. Suffice it to note here that stabilization of a triplet ground state in the presence of a quinone functionality is not as favorable for curved graphenes as it is for flat ones. Both the 9,0- and 10,0-CNT ($C_{36}H_{14}O$ and $C_{40}H_{18}O$) converge to a singlet much more readily than to a triplet. The same is true, surprisingly (based on a comparison with the corresponding flat graphene clusters), for the 9,0-CNTs containing one or two adjacent quinone functionalities with their corresponding H-free (and presumably carbene-type) active sites. The reasons for these differences are the subject of our ongoing research.

4. Summary and Conclusions

The chemical nature of carbon atoms at graphene edges and at nanotube ends, as well as at various types of defects within the basal plane of sp^2-hybridized carbon materials, has been clarified. The basal-plane sites are neither as inert as previously held[3,13,15] nor as (re)active as boldly postulated in some of the recent nanotube literature:[58] their activity is limited to providing a "reservoir" of mobile but nondesorbable carbon−oxygen surface complexes (e.g., of the epoxide type) that are crucial for eventual desorption of CO_2 from graphene edges. Oxygen insertion (graphene unzipping) and its desorption as CO_2 is favored at oxygen-saturated edges, thus accounting for the well-documented phenomenon of induced heterogeneity of carbon surfaces. Now that experimentally meaningful and thermodynamically feasible pathways to CO_2 formation have been formulated, a fruitful kinetic analysis will allow us to identify the evolution of reaction products as well as the changes in (re)active site concentration with reaction conditions, whose experimental determination has been moderately successful[53] but is often tedious.[59]

Acknowledgment. Collaboration of Dr. Kristina Skokova in the early stages of this study, as well as that of Nicolás F. Diaz Pérez and Álvaro Silva Villalobos in its final stages, is much appreciated. Financial support was provided by FONDECYT-Chile, projects 1060950, 1080334, and CCTE-UDT (CONICYT financiamiento basal).

Supporting Information Available: Coordinates of optimized geometries of all the model clusters discussed, including their absolute energies (in hartrees), complete ref 17, and charge and spin density distributions and 3D renditions of selected graphene clusters (Figures S1−S3). This material is available free of charge via the Internet at http://pubs.acs.org.

JA904731Q

(53) Lizzio, A. A.; Jiang, H.; Radovic, L. R. *Carbon* **1990**, *28*, 7–19.
(54) Johnson, J. L. *Kinetics of Coal Gasification: A Compilation of Research*; Wiley: New York, 1979.
(55) Yamashita, H.; Yamada, H.; Kyotani, T.; Radovic, L. R.; Tomita, A. *Energy Fuels* **1993**, *7*, 85–89.
(56) Illán-Gómez, M. J.; Linares-Solano, A.; Radovic, L. R.; Salinas-Martínez de Lecea, C. *Energy Fuels* **1996**, *10*, 158–168.
(57) Treptau, M. H.; Miller, D. J. *Carbon* **1991**, *29*, 531–539.
(58) Banerjee, S.; Kahn, M. G. C.; Wong, S. S. *Chem.—Eur. J.* **2003**, *9*, 1899–1908.
(59) *Fundamental Issues in Control of Carbon Gasification Reactivity*; Lahaye, J., Ehrburger, P., Eds.; Kluwer Academic Publishers: Dordrecht, The Netherlands, 1991.